

Moving Finite Element Simulation of Various Fracture Path Prediction in Materials Containing Holes and Inclusions

Nishioka T.¹, Masugami M.¹ and Fujimoto T.¹

Summary

In this paper, the simulations of fatigue crack propagation and dynamic fracture path prediction are carried out for specimens containing circular holes or inclusions, using the moving finite element method based on Delaunay automatic triangulation. And, we compared the numerical results with the experimental results.

Introduction

There is a bolt uniting in one of the main methods of uniting materials for the construction of the structure etc. 80 percent of the failure accidents that occur in complex structures that have such holes are caused by the fatigue fracture. Afterwards, the fatigue crack caused by some causes changes to the brittle fracture. That is, we need to know both fatigue fracture path and dynamic fracture path to evaluate health.

In this study, we carried out fatigue and dynamic fracture path prediction simulation containing circular holes or inclusions in materials. And this existence examined the effect on the crack growth. The former of this paper part treats fatigue fracture problem, and the latter part treats dynamic fracture problem.

The simulation was conducted using the moving finite element method based on Delaunay automatic triangulation [1,2], and the numerical results were compared with the each experiment results. In the fatigue fracture path prediction simulation, Paris's law was used to decide crack propagation length Δa and fracture-path prediction procedure was used to decide crack propagation direction. In dynamic fracture path prediction simulation, Mixed-Phase fracture path prediction mode simulation [3] that using crack velocity history that obtained by the experimental result and fracture path prediction procedure was used to reproduce.

Dynamic J Integral

To evaluate the various fracture mechanics parameters for a crack subjected to an impact stress-wave loading, and to be able to model a dynamically kinking as well as dynamically curving crack, the path independent dynamic J integral derived by Nishioka and Atluri [4] is used.

In most numerical analyses, the dynamic J integral (J') is evaluated by

$$J'_k = \int_{\Gamma+\Gamma_c} [(W+T)n_k - t_i u_{i,k}] ds + \int_{V_\Gamma} [\rho \ddot{u}_i u_{i,k} - \rho \dot{u}_i \dot{u}_{i,k}] dV \quad (1)$$

¹Structural Strength Simulation Engineering Laboratory, Faculty of Maritime Sciences, Kobe University, 5-1-1 Fukae Minamimachi, Higashinada-ku, Kobe, 658-0022, Japan

where W and T and the strain and kinetic energy densities, respectively.

The crack tip which approaches the circular holes or inclusions make it very difficult to accurately evaluate fracture parameters such as the dynamic J integral evaluation method using continuous function s is derived as follows:

$$J'_k = \int_{\Gamma+\Gamma_c} [(W+T)n_k - t_i u_{i,k}] s ds + \int_{V_\Gamma} [(\rho \ddot{u}_i u_{i,k} - \rho \dot{u}_i \dot{u}_{i,k}) s + \sigma_{ij} u_{i,k} s_{,j} - (W+K)s_{,k}] dV \quad (2)$$

where s is a continuous function defined in V_Γ . In this technique, continuous function s is defined on each point in the material, and the dynamic J integral is evaluated by the product of this s and calculation term. Equation (2) agrees with the conventional evaluation of dynamic J integral, when all s is made to be 1 in V . And, it agrees with the equivalent domain integral method, when s is made to be $s=0$ on Γ and $s=1$ in the V_Γ inside. In equation (2), when the circular holes or inclusions are included in region V_Γ , we set the s function to be $s=1$ for all of points in the domain except the circular holes or inclusions where the value is set to $s=0$, and vice versa. Hence, it is possible to easily obtain the dynamic J integral for crack tip approaching the circular holes or inclusions.

Fatigue Fracture Problem

In this part, we show study of fatigue fracture problem in the material including circular holes or inclusions. And the experimental result compared with the result of simulation. Fig.1 shows the figure of the specimen configuration used in the experiment and the simulation. The material is aluminum alloy (Al5052-H112). In the numerical simulation for fracture in the reinforced specimen, redid material is occupied in the specimen instead of circular holes. The main part of material property of the aluminum alloy is as follows: Young's modulus, $E=70.3\text{GPa}$, Poisson's ratio, $\nu=0.33$. The material property of the inclusions is as follows: Young's modulus, $E'=100E$, Poisson's ratio, $\nu=0.33$.

Fig.2 shows the profile of displacement in this experiment. The displacement is as follows: Height of specimen, $H=150$ (mm), the maximum displacement, $\bar{u}_{\max}=H/400$, the minimum displacement, $\bar{u}_{\min}=H/1200$, average displacement, $\bar{u}_m=H/600$. The speed of the repeated displacement was 20 Hz and the sine wave displacement was applied equally in the whole specimen.

In the simulation, the analysis condition was static load static analysis. A displacement-controlled load was applied. And we assume plane stress condition. Crack propagation length da/dN was decided by Paris's law that shown equation (3).

$$\frac{da}{dN} = C(\Delta K)^m \quad (3)$$

Here, C and m is constant. And we assumed that $C=1.0 \times 10^{-38}$ and $m=4$ [5].

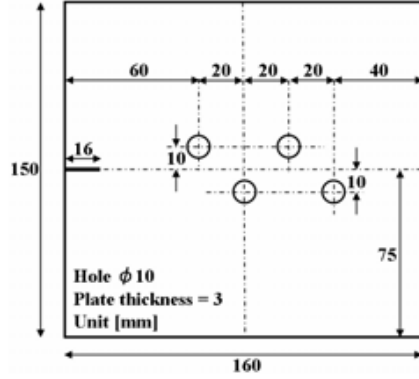


Figure 1: Shape of Specimen

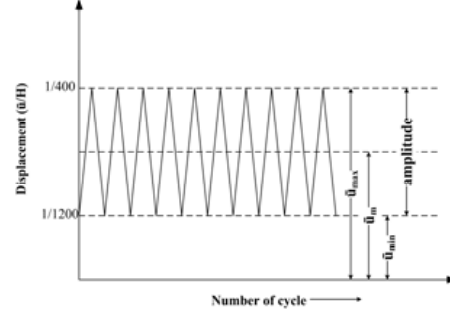


Figure 2: Loading Sequence (Displacement Control)

The value of C did the approximation evaluation from the experiment result. In the simulation, the number of repeated loading par step was 100,000 cycle. The caused stress intensity factor increases as the crack progresses. Therefore the range of effective stress intensity factor ΔK was calculated according to the following procedure. ΔK is difference between the stress intensity factor at the maximum displacement $K_{I_{\max}}^n$ and the stress intensity factor at the minimum displacement $K_{I_{\min}}^n$ in each step. ΔK at the n step is shown $\Delta K^n = K_{I_{\max}}^n - K_{I_{\min}}^n$. Here, each stress intensity factors were estimated by using J integral that calculated by using equation (2) and the component separation method [6]. Crack propagation direction was predicted by using local symmetry criterion [7] that is fracture-path prediction procedure. This theory supposes that crack grows in the direction in which the stress intensity factor K_{II} is equal to zero after the crack growth by a small increment.

Analytical procedure of this simulation at the n step is as follows:

- (i) Constrained displacement is \bar{u}_{\max} . And tentative Δa is found by using ΔK^{n-1} at the $n-1$ step and equation (3). Tentative crack propagation direction θ is found by using the maximum hoop stress ($\sigma_{\theta\theta \max}$) criterion [8]. Under maximum constrained displacement \bar{u}_{\max} , crack tip propagates to the direction θ , which determined by the maximum hoop stress criterion. And maximum stress intensity factor $K_{I_{\max}}^n$ is derived from the numerical results for crack propagation with Δa and θ .
- (ii) Under minimum constrained displacement \bar{u}_{\min} , minimum stress intensity factor $K_{I_{\min}}^n$ is derived from the way similar to (i).
- (iii) ΔK^n is determined by the $K_{I_{\max}}^n$ and $K_{I_{\min}}^n$ as (i) and (ii). ΔK^n is substituted for equation (3) and calculated Δa^n . Then under average constrained displacement \bar{u}_m , crack is propagated to the direction of K_{II} equal 0.

We calculated (iii) from (i) repeating each step severally and carried out fatigue fracture path prediction simulation.

Dynamic Fracture Problem

In this part, we show study of dynamic fracture problem in the material including circular holes or inclusions, and the experimental result compared with the result of simulation in order to evaluate the accuracy of the simulation using this technique. In this simulation, crack propagation velocity was used experimental result. Fig.3-(a) shows the figure of the specimen configuration used in the experiment and the simulation. And the initial mesh pattern of simulation is shown in Fig.3-(b). The material is PMMA. In the numerical simulation for fracture in the reinforced specimen, redid material is occupied in the specimen instead of circular holes as well as fatigue fracture path prediction simulation. The main part of material property of the PMMA is as follows: Young's modulus, $E=2.95\text{GPa}$, Poisson's ratio, $\nu=0.3$. The material property of the inclusions is as follows: Young's modulus, $E'=206\text{GPa}$, Poisson's ratio, $\nu=0.28$.

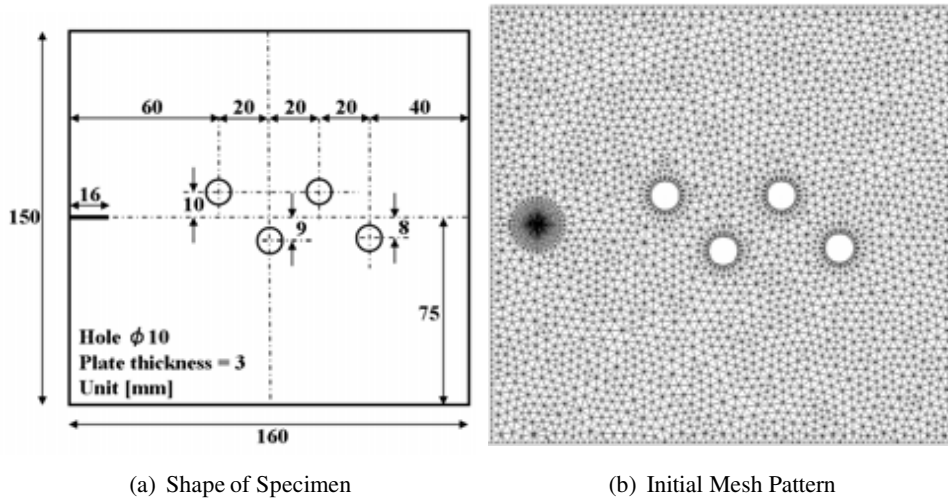


Figure 3: Simulation geometry

In the simulation, the analysis condition was static load dynamic analysis. A displacement-controlled load was applied. And we assume plane stress condition. Crack propagation direction was predicted by using local symmetry criterion.

Numerical result

Fig.4 shows the fatigue fracture path obtained from the numerical simulation and the experiment. In the multiple holes problem, both the experimental result and the simulated result, while crack tip is approaching the first circular hole, the crack tip progresses as if it is attracted to the hole. No sooner the crack tip had passed

the first circular hole than the effect that is attracted to the second circular hole becomes intense. So the crack tip changes the direction and progresses while meandering. In the other case of multiple inclusions problem, crack tip progresses like avoiding inclusions. A similar result was derived about the dynamic fracture path obtained from the numerical simulation and the experiment. The dynamic fracture path is shown in Fig.5. In the multiple holes problem, the simulated fracture path corresponds to the experimental fracture path very well.

In addition, as for each point that shows fracture path of Fig.4, crack tip position history is plotted at intervals of three steps (300,000 cycle). From the simulation result, in the multiple holes problem, the crack propagation velocity becomes fast while the crack tip is approaching circular holes and becomes slow while going away. In the other case of multiple inclusions problem, inclusions don't have the influence too much for the crack propagation velocity.

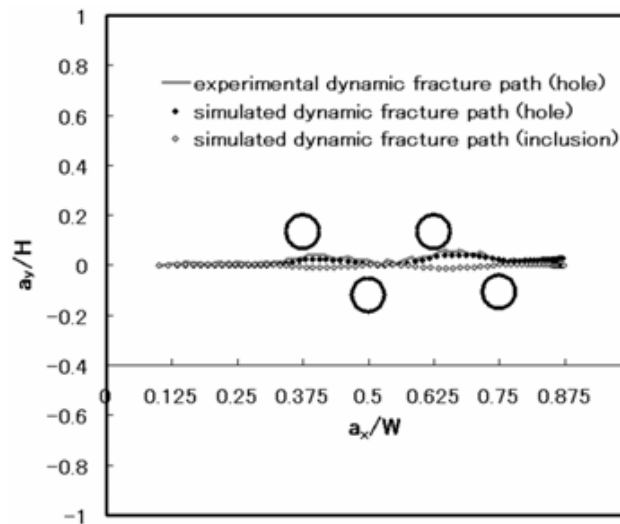


Figure 4: Numerical-Experimental Dynamic fracture path

Fig. 6 shows the stress intensity factor K_I that obtained by the fatigue fracture path prediction simulation. 4 circles in the figure express the place when crack tip propagated center coordinate of each circular holes or inclusions. In the multiple holes problem, K_I value is increasing while crack tip is approaching circular holes, and K_I value is decreasing while going away from circular holes. In the other case of multiple inclusions problem, K_I value is decreasing while crack tip is approaching inclusions, and K_I value is increasing while crack tip is going away from inclusions. A similar result was derived about the numerical result of dynamic fracture path prediction simulation. Thus it was understood that circular holes or inclusions

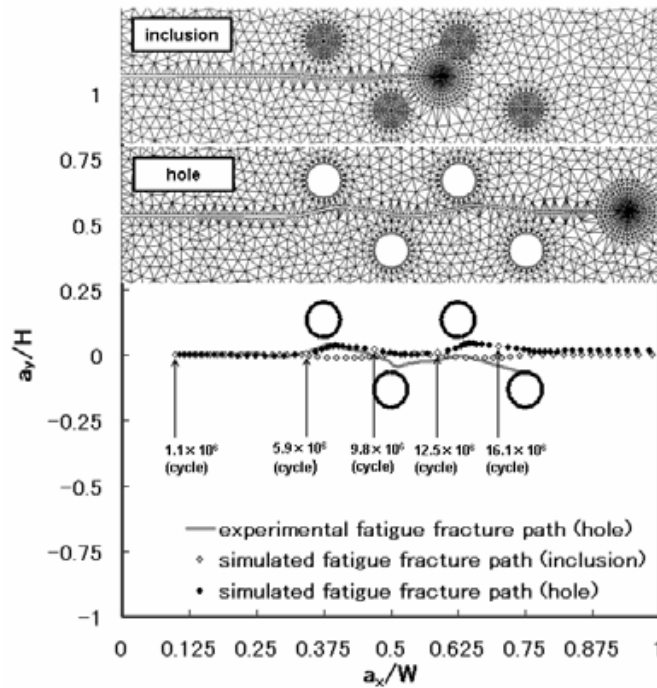


Figure 5: Numerical-Experimental Fatigue Fracture Path

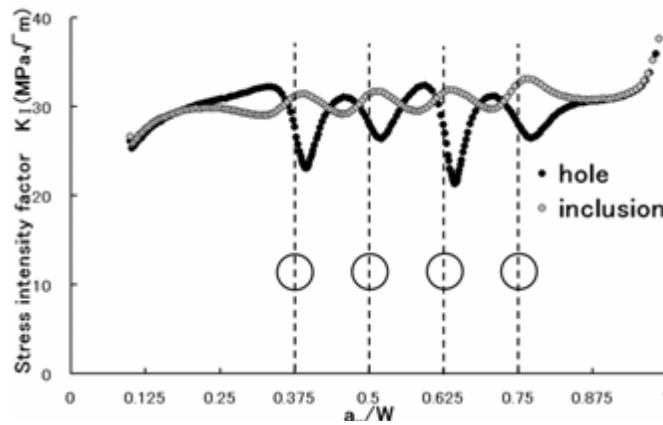


Figure 6: History of Stress Intensity Factor

in the material strongly influence K_I value when the crack is propagating.

Conclusions

It is understood that in the materials containing circular holes or inclusions, when crack is propagating, fracture path and stress intensity factor K_I strongly

receive the same influence from circular holes or inclusions even if it is fatigue fracture or dynamic fracture. Moreover, it is understood that in the multiple holes problem, crack propagation velocity also strongly receive the influence of circular holes from the numerical result of the fatigue crack propagation prediction simulation.

References

1. Sloan, S.W. and Houlsby, G.T. (1984): "An Implementation of Waston's Algorithm for Computing 2-Dimensional Delaunay Triangulations", *Advances in Engineering Software*, Vol. 6, pp. 192-197.
2. Taniguchi, T. (1992): *Automatic Mesh Generation for FEM: Use of Delaunay Triangulation*, Morikita Publishing, (Japanese).
3. Nishioka, T., Hybrid numerical methods in static and dynamic fracture mechanics, *Optics and Laser Engineering*, 32-3, (2000), pp.205-255.
4. Nishioka, T. and Atluri, S.N. (1983): "Path Independent Integrals, Energy Release Rates, and General Solutions of Near-Tip Fields in Mixed-Mode Dynamic Fracture Mechanics", *Eng. Fract. Mech.*, Vol.18, No.1, (1983), pp.1-22.
5. Yagawa, M. (2004): *Structural Engineering Handbook*, pp.199, (Japanese).
6. Nishioka, T., Murakami, R. and Matsuo, S., *Computational Mechanics '91, ICES Publications*, (1991), pp.750-775.
7. Goldstein, R.V. and Salganik, R.L. (1974): "Brittle Fracture of Solids with Arbitrary Cracks", *Int. J. Fract.*, Vol.10, No.10, pp.507-523.
8. Erdogan, F. and Sih, G.C. (1963): "On the Crack Extension in Plates under Plane Loading and Transverse Shear", *Journal of basic Engineering, ASME*. Vol.85, pp.519-527.

